International Journal of Physics and Mathematics

E-ISSN: 2664-8644
P-ISSN: 2664-8636
IJPM 2025; 7(1): 30-40

www.physicsjournal.net
Received: 02-01-2025
Accepted: 05-02-2025

Hanaa Mohammed Hadad
Department of Physics, College of Science, Thi-Qar University, Thi-Qar, Iraq

Abbas Shwya Alwan
Department of Physics, College of Science, Thi-Qar University, Thi-Qar, Iraq

Corresponding Author:
Abbas Shwya Alwan
Department of Physics, College of Science, Thi-Qar University, Thi-Qar, Iraq

Studying the electronic properties and adsorption of zinc oxide (ZnO) and iron disulfide (FeS_2) on the surfaces of ($3CaTiO_3$) and ($3CaTiO_3/TiO_3$)

Hanaa Mohammed Hadad and Abbas Shwya Alwan

DOI: https://www.doi.org/10.33545/26648636.2025.v7.i1a.104

Abstract
Density functional theory have been submitted at the basis sets 6-31G, B3LY by utilizing quintessential algorithms in Gaussian 09 package to study the adsorption procedure of zinc oxide (ZnO) and iron disulfide (FeS_2) on the nanomaterial surfaces **(**$3CaTiO_3$) and **(**$3CaTiO_3/TiO_3$). The molecular geometry, the electrostatic potential (ESP), density contour maps, infrared spectra (IR), density of states have been investigated. The following calculations: HOMO energy, LUMO energy, energy gap, average polarizability, dipole moment, ionization potential and electron affinity have been held. The highest value of dipole moment (μ) was as a result to adsorption procedure of FeS_2 on the nanomaterial surface **(**$3CaTiO_3$), (μ=24.238648 Debye), the substances that have dipole moment consider have importance in the branch of knowledge the optics. The values of energy gap for all nanomaterial structures were in the range of semiconductor materials. The nanomaterial structures ($3CaTiO_3$)-ZnO and ($3CaTiO_3$)-FeS_2 have energy gap approximately (0.30 eV), this value close to the energy gap of lead telluride (PbTe). The scientists utilize lead telluride (PbTe) as one of semiconductor materials to convert the heat to electronic energy. The nanomaterial structure ($3CaTiO_3$)-ZnO owns the maximum value of polarizability, ($\langle\alpha\rangle$ =934.488129 a.u). All nanomaterial structures have the identity and mirror plane because they have the point group symmetry (C_S / C_1), therefore one can say this symmetry merit of the nanomaterial structures make them have significance in the optics devices. Density of states diagrams demonstrates new energy levels can be occupied by electrons after the adsorption procedure.

Keywords: DFT, adsorption, energy gap, infrared spectra, polarizability.

Introduction
In physics, chemistry, and material reresearches, density functional theory (DFT) is a computational quantum mechanical modeling technique used to examine the electronic structure (mostly the ground state) of numerous systems, specifically molecules, atoms, and condensed phases [1, 2]. According to this theory, functional is a functions of another functions. The spatially electron density can be employed to determine the features of a multiple electron system [3]. DFT is one of the most widely used and adaptable techniques in computational physics, computational chemistry, and condensed-matter physics [4]. Since the 1970s, DFT has been widely employed for solid state physics computations [5]. DFT is utilized for holding calculations of the many electron systems with dependence on the electron density rather the wave function [6]. There are many researchers prove that the evaluations of DFT agree satisfactorily with the evaluations of the experiments [7]. DFT was presented by the scientists Hohenberg-Kohn in 1964 and Kohn-Sham in 1965 in two scientific papers, the scientists Thomas and Fermi were the predecessor of this method (DFT) [8]. DFT implies many exchange correlation functions, just like local density approximation (LDA), local spin density approximation (LDA) and generalized gradient approximation (GGA). Those exchange correlation functions make the evaluations of DFT more accurate [9]. The calculations of DFT to become more accurate also utilizes basis sets. The basis sets typify a combination of functions describe the atomic orbitals, in which the linear combination of the atomic orbitals yields a molecular orbital [10]. One of the basis sets that employed profoundly with DFT is 6-31G (split valence basis set). This basis set utilize six Gaussian orbitals to the inner core, three Gaussian orbitals to the inner valence, but one Gaussian orbital to the outer shell [11]. So the hybrid functional B3LYP is one of the most functionals that is employed with DFT, this technique was introduced by at first by Axel Becke in 1993 to describe the energies of exchange-correlation [12]. Density functional theory (DFT)

utilizes quintessential algorithms in Gaussian 09 and Gauss view 06 to obtain the consequences [13]. DFT divides the energy into partitions: electronic kinetic energy, electron-nuclear attractions and electron electron repulsion [14]. The scientist John Polple in 1998 was given Nople prize in chemistry in appreciation to his efforts in sophistication DFT calculations [15]. Perovskite ($CaTiO_3$) is a material that has a special crystal structure. Several reresearch groups have created photovoltaic perovskites that are similar to many of these commercial solar cells. Perovskites are more effective than silicon in converting some parts of the light spectrum into electricity and vice versa. Therefore, the effectiveness of employing perovskite comes through its contribution to increasing energy production in the majority of solar cells and thus integrating it with silicon, not replacing it [16]. Zinc oxide (ZnO) is an inorganic material with white color [17]. Some of the most importance applications of zinc oxide as a nanomaterial are electronic devices and gas sensors [18]. Iron disulfide has the chemical formula (FeS_2) nanomaterial has importance in the manufacture of photo-electric cells, light detectors, rechargeable batteries and light motivation [19].

Results and Discussion

Molecular Geometry

The molecular geometry considers the base that the chemistry depends on for studying the changes that occur in the materials [20]. The molecular geometry of the molecules consists of linkage the atoms one another physically and chemically. The molecular structure consists of number of different atoms connect one another in which they appear practically as one particle. Generally, when the atoms close one another, there are three probabilities result, either ionic bond or covalent bond or there is no bond. If there is no bond result, the system will be unstable [21]. The molecular structure for **(**$3CaTiO_3$), **(**$3CaTiO_3/TiO_3$), **(**$3CaTiO_3$)-ZnO, **(**$3CaTiO_3$)-FeS_2, **(**$3CaTiO_3/TiO_3$)-ZnO and **(**$3CaTiO_3/TiO_3$)-FeS_2 systems have been submitted by utilization density functional theory (DFT) technique at the basis sets 6-31G and B3LYP throughout sophisticated algorithms in Gaussian09 (G09) package.

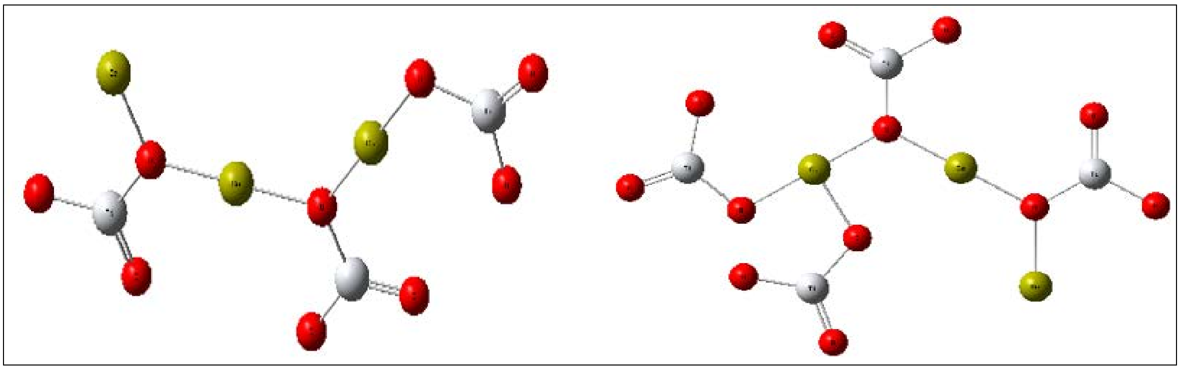

(a) ($3CaTiO_3$) (b) ($3CaTiO_3/TiO_3$)

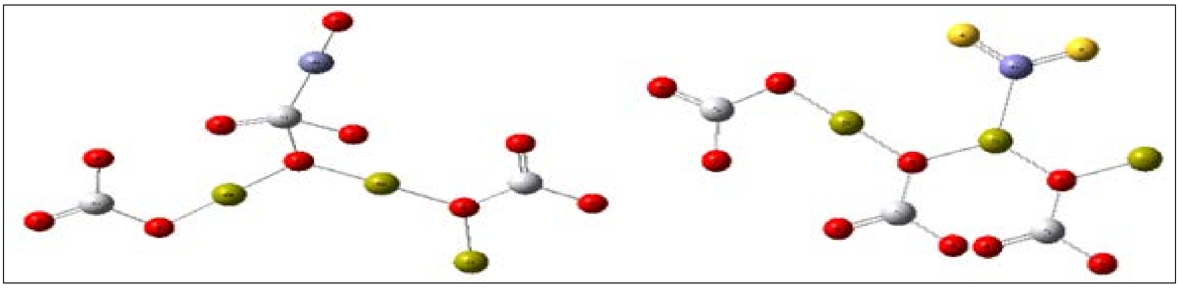

(c) ($3CaTiO_3$)-ZnO (d) ($3CaTiO_3$)-FeS_2

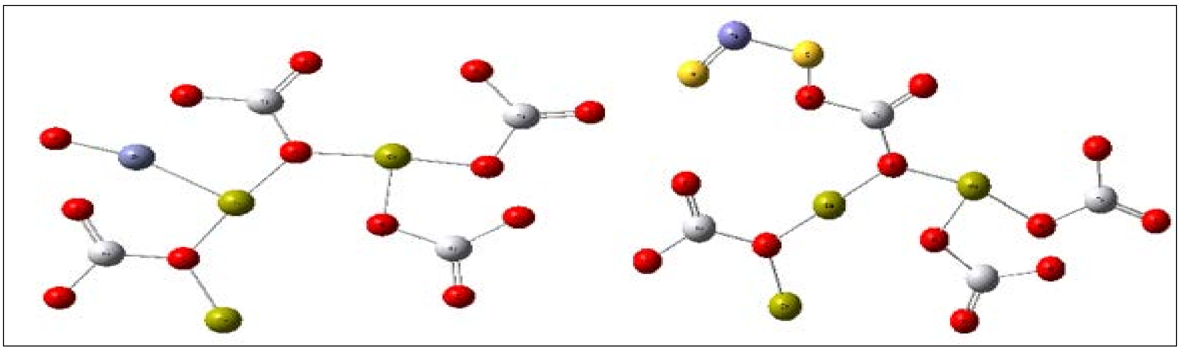

(e) ($3CaTiO_3/TiO_3$)-ZnO (f) ($3CaTiO_3/TiO_3$)-FeS_2

Fig 1: The molecular structure for a.**(**$3CaTiO_3$), b.**(**$3CaTiO_3/TiO_3$), c.**(**$3CaTiO_3$)-ZnO, d.**(**$3CaTiO_3$)-FeS_2, e.**(**$3CaTiO_3/TiO_3$)-ZnO and f.**(**$3CaTiO_3/TiO_3$)-FeS_2 systems.

Figure (1) depicts the atoms with bronze color typify calcium atoms, the atoms with light lead color represent titanium, the atoms with red color stand for oxygen, the atoms with yellow color represent sulfur atoms, the atoms with light blue color typify the iron atoms, but the atoms with lead color stand for zinc atoms. The molecular geometry can be obtained computationally or tentatively, it is regarded reference of the information about the physical and chemical merits of the molecule. The molecular geometry links profoundly with it's electronic structure. The data of rotational spectra analysis give the rotational constants of the molecules, which permit to renew the principal moments of inertia and eventually the molecular geometry. The bonds in poly atomic molecules in general are more complicated than there are bonds. In fact, they will be more complicated of that but for rapprochement one another impact only to the outer shells. The reason here be the electrons in the inner shell be binding more with the nucleus. Another reason is the inner shells remains far one another even where the atoms reach to the minimum distance one another.

Electrostatic Potential (ESP)

The term electrostatic potential describes the possibility of the system or the molecular geometry to exert work. So the system consists of charged particles interact through electrostatic forces. Either the electrostatic potential sometimes be expressed the collection energy of the charges. With other words the electrostatic potential is a physical merit equal in scalar the electrostatic energy among the static charge distribution of an atomic or molecular system and positive point charge locate at distance of it [22]. The electrostatic potential (ESP) for **(**$3CaTiO_3$), **(**$3CaTiO_3/TiO_3$), **(**$3CaTiO_3$)-ZnO, **(**$3CaTiO_3$)-FeS_2, **(**$3CaTiO_3/TiO_3$)-ZnO and **(**$3CaTiO_3/TiO_3$)-FeS_2 systems have been achieved by utilization density functional theory (DFT) technique at the basis sets 6-31G and B3LYP throughout quintessential algorithms in Gaussian09 (G09) package.

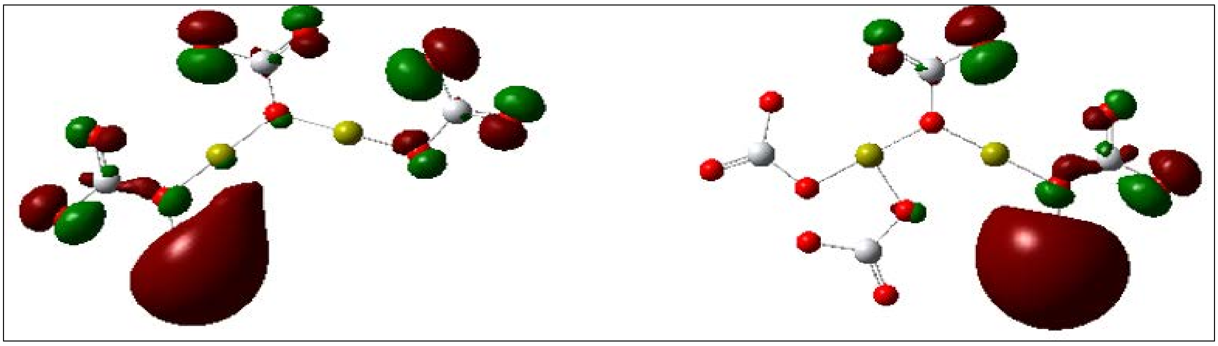

(a) ($3CaTiO_3$) **(b)** ($3CaTiO_3/TiO_3$)

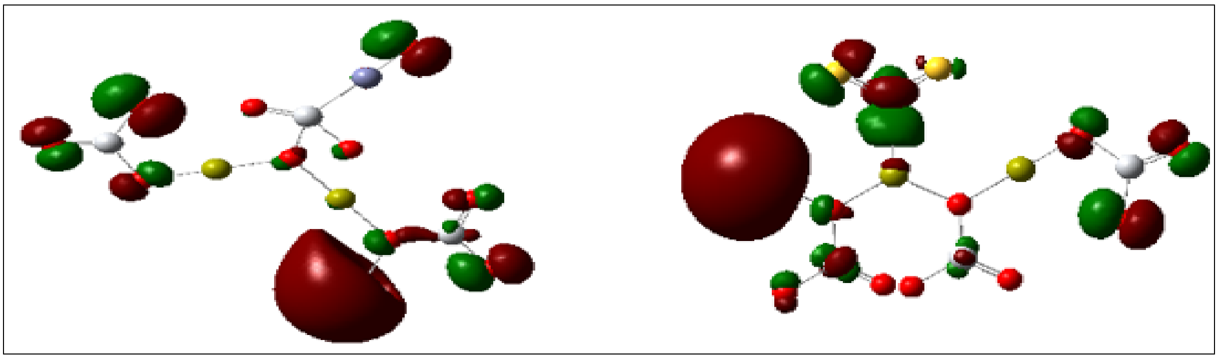

(c) ($3CaTiO_3$)-ZnO **(d)** ($3CaTiO_3$)-FeS_2

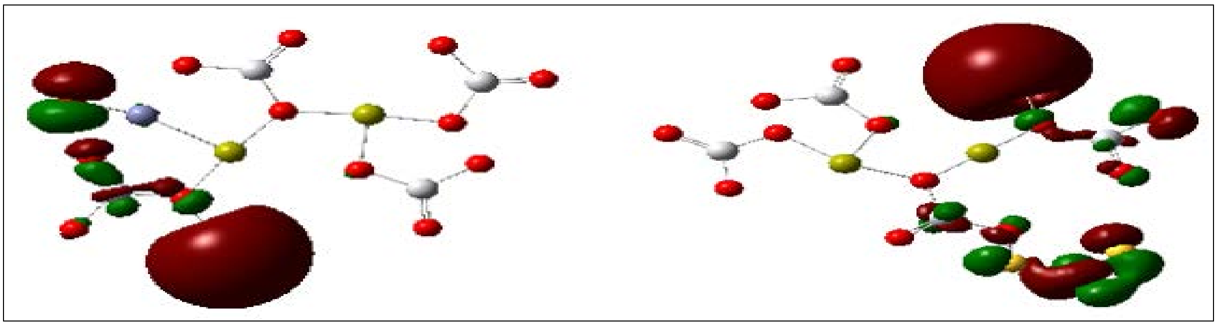

(e) ($3CaTiO_3/TiO_3$)-ZnO **(f)** ($3CaTiO_3/TiO_3$)-FeS_2

Fig 2: The electrostatic potential for a.**(**$3CaTiO_3$), b.**(**$3CaTiO_3/TiO_3$), c.**(**$3CaTiO_3$)-ZnO, d.**(**$3CaTiO_3$)-FeS_2, e.**(**$3CaTiO_3/TiO_3$)-ZnO and f.**(**$3CaTiO_3/TiO_3$)-FeS_2 systems.

Figure (2) clarifies the electronic charge distribution around the nucleus of the atoms. One can visualize that the adsorption procedure of FeS_2 on the nanomaterial surface **(**$3CaTiO_3$) makes the concentration of the charges density in the vicinity region between calcium in **(**$3CaTiO_3$) and iron atom, sulfur atom. Either charges density concentration around the atoms of iron and sulfur and calcium appears in vicinity region among them as a result to the adsorption procedure. One can visualize the nucleus sends positive test charge on the on the surface to interact with the electronic charges. The high electrostatic potential point out stronger positive charge. The electrostatic potential schematics give the charge distribution in three dimensions and also describe mechanism of atoms interaction one another. So the electrostatic potential diagrams predict to behavior of the complex molecules. The maroon color indicates to the lowest value of energy, but the green color refers to the highest value of energy.

Contours

The contour map is a term express on the density of electronic charges. Contour maps also describe the mechanism of interaction through clarification the active regions in the molecular geometry, and also interpret many of phenomena just like charge transfer, charge exchange between the atoms, ions with surfaces. Charge distribution in space is also can be expressed by utilization density contour maps [23]. The contour curves for **(**$3CaTiO_3$), **(**$3CaTiO_3/TiO_3$), **(**$3CaTiO_3$)-ZnO, **(**$3CaTiO_3$)-FeS_2, **(**$3CaTiO_3/TiO_3$)-ZnO and **(**$3CaTiO_3/TiO_3$)-FeS_2 systems have been investigated by employment density functional theory (DFT) technique at the basis sets 6-31G and B3LYP throughout developing algorithms in Gaussian09 (G09) package.

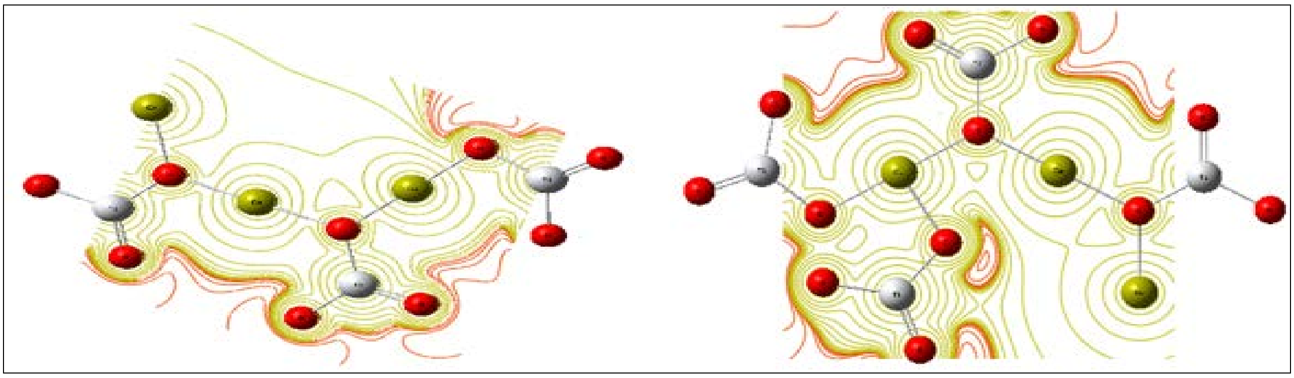

(a) ($3CaTiO_3$) **(b)** ($3CaTiO_3/TiO_3$)

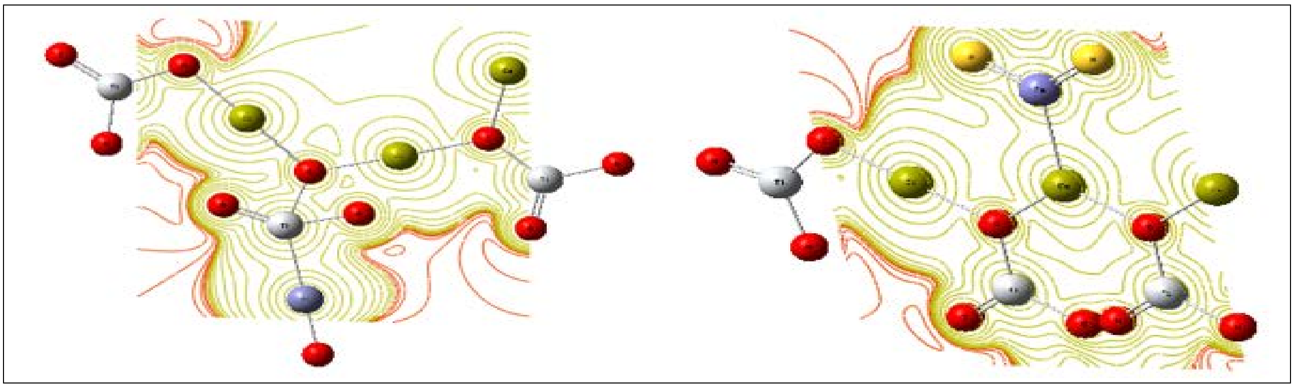

(c) ($3CaTiO_3$)-ZnO **(d)** ($3CaTiO_3$)-FeS_2

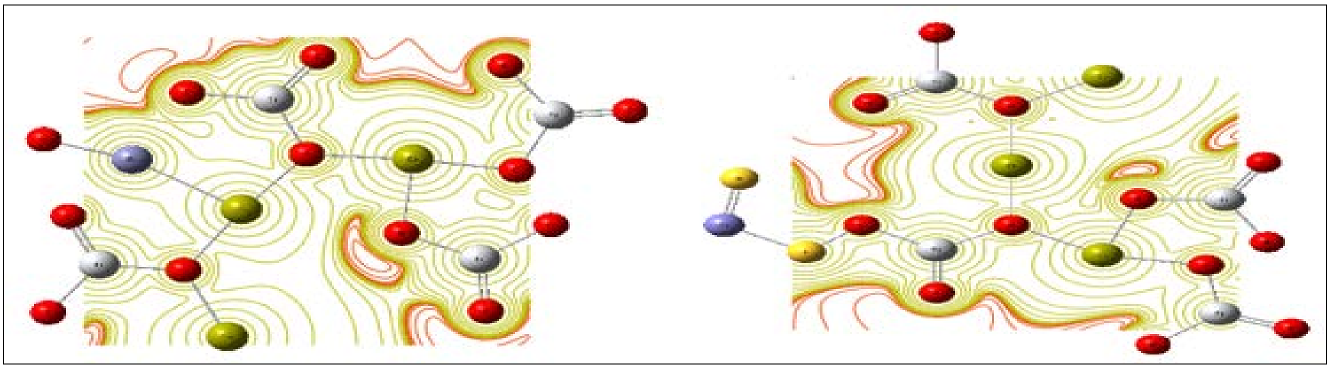

(e) ($3CaTiO_3/TiO_3$)-ZnO **(f)** ($3CaTiO_3/TiO_3$)-FeS_2

Fig (3): The density contour maps for a.**(**$3CaTiO_3$), b.**(**$3CaTiO_3/TiO_3$), c.**(**$3CaTiO_3$)-ZnO, d.**(**$3CaTiO_3$)-FeS_2, e.**(**$3CaTiO_3/TiO_3$)-ZnO and f.**(**$3CaTiO_3/TiO_3$)-FeS_2 systems.

Figure (3) illustrates that adsorption of the molecules FeS_2 and ZnO on the surfaces of ($3CaTiO_3$) and **(**$3CaTiO_3/TiO_3$) leads to distortion in the density contour maps around the atoms. The contour maps describe Fermi surface, Fermi surface is very important to give interpretation to many of phenomena, especially solid state physics. The electrons movement in the contour curves is not constrained in the regions far from Brillion zones, but the convergence to Brillion zone the contour map curves finish at the boundaries of these zones, whereas the contour maps typifies energy curves. The electrons cannot pass through from the first Brillion zone to the second Brillion zone unless they acquire energy enough to pass through the energy gap between the two zones. One can visualize as a result to the adsorption procedure of ZnO on the nanomaterial surface ($3CaTiO_3/TiO_3$), there is contour circles form about the zinc atom systematically. So the adsorption procedure of FeS_2 on the nanomaterial surface ($3CaTiO_3/TiO_3$) depicts the contour circles form about the iron atom systematically. The adsorption procedure of FeS_2 on the nanomaterial surfaces ($3CaTiO_3$) and ($3CaTiO_3/TiO_3$) shows systematic charge distribution around the two sulfur atoms. The adsorption procedure of ZnO on the nanomaterial surface ($3CaTiO_3$) leads to regular charge distribution of electronic charges around the zinc atom.

Electronic states: The electronic states can be described through energy levels that perhaps be occupied with electrons. The HOMO and LUMO energies describe the energies in the highest occupied orbit with one electron or two electrons and the energies in the lowest occupied orbit with one electron or two electrons respectively. The energy difference between them yield electronic band gap (E_g). According to band theory in solid state physics there are two bands one of them be full with electrons, but the other be empty of electrons, energy gap separate them. The width of this gap is different according to the material if it is semiconductor or conductor or insulator. Mathematically the band gap width is given by the equation [24].

$$E_g = E_{LUMO} - E_{HOMO} \quad (1)$$

Table 1: The electronic states and energy gap (E_g) for ($3CaTiO_3$), ($3CaTiO_3/TiO_3$), ($3CaTiO_3$)-ZnO, ($3CaTiO_3$)-FeS_2, ($3CaTiO_3/TiO_3$)-ZnO and ($3CaTiO_3/TiO_3$)-FeS_2 systems.

System	E_{LUMO} (eV)	E_{HOMO} (eV)	E_g (eV)
($3CaTiO_3$)	-5.5921992	-5.8961349	0.303936
($3CaTiO_3$)-ZnO	-5.5483911	-5.8506942	0.302303
($3CaTiO_3$)-FeS_2	-4.8956232	-5.2221432	0.32652
($3CaTiO_3/TiO_3$	-5.7660711	-6.154902	0.388831
($3CaTiO_3/TiO_3$)-ZnO	-5.6784549	-6.1989822	0.520527
($3CaTiO_3/TiO_3$)-FeS_2	-4.7960346	-5.1282687	0.332234

One can watch in the table (1) the energies of HOMO and LUMO which have the significance in the theory of molecular orbitals, whereas the combination (linear) of the atomic orbitals yield molecular orbitals. They describe the boundaries molecular orbitals that have significance in the determination of optical and electronic characteristics of the molecules. When the electron gains an energy transport from HOMO to LUMO. The energy HOMO describe the molecule ability for donation by electrons. The adsorption of FeS_2 on the nanomaterial surface make it the best donor because ($3CaTiO_3/TiO_3$)-FeS_2 owns the lowest numerical value of HOMO energy, the value is (-5.1282687 eV). Table (1) also summarizes the values of energy gaps in the domain between approximately (0.30 eV) to (0.52 eV). All those values of energy gaps are in the range of semiconductor materials which have number of different applications in many of electronic devices. The adsorption procedure of FeS_2 and ZnO on the surface of ($3CaTiO_3$) yields values of energy gaps close to (0.30 eV), this value of energy gaps closes to the energy gap of lead telluride (PbTe). This make it a semiconductor nanomaterial recognizes by excellent performance in the intermediate temperatures. lead telluride (PbTe) be utilized to convert the heat to electronic energy, one can say it has thermo electric merits.

Polarizability

The polarizability term is utilized to describe the molecules tendency to enhance dipole moment of an electric field that has been originated by another molecule. The polarizability is a tensor quantity dependently on value of the dipole moment. In other words, the polarizability stands for the resultant moments of dipoles per unit volume. The polarizability tensor elements depend on the derivative of second order to the energy in Cartesian coordinates. Mathematically the polarizability in Cartesian coordinates can be expressed by the equation[25].

$$\alpha_{i,j} = \frac{\partial^2 E}{\partial F_i \, \partial F_j} \quad (2)$$

The symbols i and j indicates to the components x and y. Let α_{xx}, α_{yy} and α_{zz} are the polarizability tensors, hence average polarizability can be expressed by the equation [26].

$$< \alpha > = \frac{1}{3}\left(\alpha_{xx} + \alpha_{yy} + \alpha_{zz}\right) \quad (3)$$

Table 2: The average polarizability for ($3CaTiO_3$), ($3CaTiO_3/TiO_3$), ($3CaTiO_3$)-ZnO, ($3CaTiO_3$)-FeS_2, ($3CaTiO_3/TiO_3$)-ZnO and ($3CaTiO_3/TiO_3$)-FeS_2 systems.

System	Average polarizability (a.u)
($3CaTiO_3$)	806.567365
($3CaTiO_3$)-ZnO	934.488129
($3CaTiO_3$)-FeS_2	905.864206
($3CaTiO_3/TiO_3$	602.470142
($3CaTiO_3/TiO_3$)-ZnO	598.009200
($3CaTiO_3/TiO_3$)-FeS_2	872.347125

Table (2) demonstrates that the adsorption of ZnO on the nanomaterial surface ($3CaTiO_3$) makes it the highest activity nanomaterial structure because ($3CaTiO_3$)-ZnO has the highest numerical value of the average polarizability, the value is approximately (934.488 a.u). The polarizability describes the charge transport among the atoms that formulate the molecular system. The polarizability is important in determination charge distribution throughout the interaction between atoms, molecules, gases on the one hand and the surfaces on the other hand. One of the applications of polarizability in optics is the optical basicity. If the electric field impact to molecules, the positive charges (cores) bias toward the electric field, while the negative charges (electrons) bias to the opposite side of the electric field direction, eventually the charges will separate one another. The polarizability depends profoundly on the molecular geometry, therefore, there is variety kinds of polarizabilities according to the composition of the polarized molecules in the substances. The polarizability has maximum significance because it provides with information about the internal atomic structure of different materials. Each type of polarizability has special credit, the binary polarizability depicts depending strongly on the temperature vise the ionic polarizability and electronic polarizability.

Dipole moment

The dipole moment originates between two charges one of them positive, but the other negative, between them displacement. Peter Debye is the first one physics scientist describes the dipole moment, and the unit (Debye) of the dipole moment take the name from this physics scientist. Generally, the dipole moment emerges in the heterogeneous molecules and influences profoundly with change of direction of the displacement. The dipole moment also emerges between the different magnetic dipoles as origination between two different electric dipoles. The magnetic dipole may be permanent or induced. The dipole moment considers a vector quantity. Suppose two charges each one of them (*q*), between them the displacement (*r*). The dipole moment can be given by the relation [27].

$$\mu = q * r \tag{4}$$

Table 3: The dipole moment for ($3CaTiO_3$), ($3CaTiO_3/TiO_3$), ($3CaTiO_3$)-ZnO, ($3CaTiO_3$)-FeS_2, ($3CaTiO_3/TiO_3$)-ZnO and ($3CaTiO_3/TiO_3$)-FeS_2 systems.

System	Dipole Moment (Debye)
($3CaTiO_3$)	22.503047
($3CaTiO_3$)-ZnO	21.338722
($3CaTiO_3$)-FeS_2	24.238648
($3CaTiO_3/TiO_3$)	21.593173
($3CaTiO_3/TiO_3$)-ZnO	19.455898
($3CaTiO_3/TiO_3$)-FeS_2	6.435441

Table (3) summarizes the numerical values of the dipole moment before and after the adsorption procedure. The adsorption procedure of FeS_2 on the nanomaterial surface ($3CaTiO_3/TiO_3$) causes decrease profoundly in the value of dipole moment. The adsorption reduces the value from (21.59 Debye) to (6.43 Debye). One can see the adsorption procedure of FeS_2 on the nanomaterial surface ($3CaTiO_3$) make it the greatest dipole moment nanomaterial structure, it is approximately about (24.23 Debye). Generally, the molecules that have dipole moment is called (polar), therefore the dipole moment is one of the important quantities in physics to distinguish between the polar bonds and nonpolar bonds. Also the dipole moment determines the degree of polarization of covalent bond and it connects profoundly to the molecular geometry of the materials. Hence, one can say the dipole moment play a vital role for determination nature of polarization and the chemical bonding. The bond polarization degree increase with the increasing of the value of dipole moment. Determination the value of dipole moment has importance in the designation of the optical devices.

Symmetry

The sphere be regarded more symmetric than the cube, the sphere repeat itself through any rotation angle, but the cube looks itself only through the rotation at determined angles around an axis. The symmetry be considered have importance for determination some physical credits without making calculations [28]. The symmetry operation is a property to the molecule or particle allows by holding transformation in which the molecule or particle remains the same (unchanged). For each symmetry operation symmetry element related to it. The symmetry operations are reflection, inversion, rotation and improper rotation [29].

Table 4: The point group symmetry for ($3CaTiO_3$), ($3CaTiO_3/TiO_3$), ($3CaTiO_3$)-ZnO, ($3CaTiO_3$)-FeS_2, ($3CaTiO_3/TiO_3$)-ZnO and ($3CaTiO_3/TiO_3$)-FeS_2 systems.

System	Point group symmetry
($3CaTiO_3$)	C_S / C_1
($3CaTiO_3$)-ZnO	C_S / C_1
($3CaTiO_3$)-FeS_2	C_S / C_1
($3CaTiO_3/TiO_3$	C_S / C_1
($3CaTiO_3/TiO_3$)-ZnO	C_S / C_1
($3CaTiO_3/TiO_3$)-FeS_2	C_S / C_1

.

Table (4) exhibits all nanomaterial structures of the type of point group symmetry (C_S / C_1). Those nanomaterial structures have plane of mirror plane and the identity, because they have the point group symmetry (Cs/C_1). This characteristics of the nanomaterial surface make it important in the optics devices. One can say the nanomaterial structures can repeat themselves each (360°), because the kind of point group symmetry (C_1), in this kind of symmetry the repetition is happening through (360°/n) around the centerpiece, in which n stands for the order of the centerpiece, here (n=1). Existence of determined symmetry element cause interchange bonds. The nanomaterial structures have the point group symmetry kind (Cs), i.e. identity. The identity can be described mathematically by unitary matrix. The identity here means do nothing but it is important. Identity describes different operations is occurring successively result from displace the molecular structure from it's original position, just like reflection followed by reflection or inversion followed by inversion. The rotation of molecule occurs through centerpiece called rotation centerpiece. The symmetry credit plays an active role in the physical properties of the molecules such as orbitals interactions in order to formation the bonds, the (allowed and permitted) translation energies, magnetic properties and optical properties. One of the most important applications to symmetry is the optical activity.

Ionization potential (I.P) and Electron affinity (E.A)

The ionization potential describes lowest energy required to displace an electron from the atom. There is ionization energy can be measured for each electron in the atom. The electron affinity describes the variety in the energy of a neutral atom through addendum an electron to the atom in order to formation negative ion [30]. The first ionization energy is the required energy to eliminate the first electron. The second ionization energy is the energy required to remove the second electron and so on [23]. According to the theory of Koopman the ionization potentials and electron affinities can be evaluated by utilization the relations [30].

$$I.P = -E_{HOMO} \tag{5}$$

$$E.A = -E_{LUMO} \tag{6}$$

Table 5: The ionization potential (I.P) and electron affinity (E.A) for ($3CaTiO_3$), ($3CaTiO_3/TiO_3$), ($3CaTiO_3$)-ZnO, ($3CaTiO_3$)-FeS_2, ($3CaTiO_3/TiO_3$)-ZnO and ($3CaTiO_3/TiO_3$)-FeS_2 systems.

System	I.P (eV)	E.A (eV)
($3CaTiO_3$)	5.8961349	5.5921992
($3CaTiO_3$)-ZnO	5.8506942	5.5483911
($3CaTiO_3$)-FeS_2	5.2221432	4.8956232
($3CaTiO_3/TiO_3$	6.154902	5.7660711
($3CaTiO_3/TiO_3$)-ZnO	6.154902	5.6784549
($3CaTiO_3/TiO_3$)-FeS_2	5.1282687	4.7960346

Table (5) demonstrates that the adsorption procedure of FeS_2 on the nanomaterial surface ($3CaTiO_3/TiO_3$) make it owns the minimum value of the ionization potential, I.P of the nanomaterial structure ($3CaTiO_3/TiO_3$)-FeS_2 is approximately (4.79 eV), hence the electrons in the nanomaterial structure ($3CaTiO_3/TiO_3$)-FeS_2 need less energy to be free and then participate active participation in the bonding with other atoms to obtain more stable nanomaterial structure. The nanomaterial structure ($3CaTiO_3/TiO_3$) is the maximum electron affinity, E.A of the nanomaterial structure ($3CaTiO_3/TiO_3$)-ZnO is approximately (6.19 eV), therefore, the unoccupied or partial occupied electronic orbitals in this nanomaterial structure be more ability to be occupied by the electrons. The ionization potential and electron affinity impact profoundly to the levels of translation and charge transfer processes. The ionization potential links to the type of shell system if it is open or close. One of the most important factors that effect on the ionization energy is shielding of electrons, i.e. the covalent electrons are shielded from the core by the inner electrons. The electron affinity is measured to each electron adding to the atom.

Density of states (DOS)

The description of density of states of the electrons in the bands is done by number of states within determined energy domain. This function (density of states) is regarded have significance in the electronic processes, especially transport phenomena. In other phrase, it can be said that the density of states typifies the number of electrons per unit volume in energetic domain. Sometimes, it is beneficial to know the density of states in the energy range that locates near the top of band near representation the band by the negative effective mass [31]. The density of states for ($3CaTiO_3$), ($3CaTiO_3/TiO_3$), ($3CaTiO_3$)-ZnO, ($3CaTiO_3$)-FeS_2, ($3CaTiO_3/TiO_3$)-ZnO and ($3CaTiO_3/TiO_3$)-FeS_2 systems have been inquired by employment density functional theory (DFT) technique at the basis sets 6-31G and B3LYP throughout sophisticated algorithms in Gaussian09 (G09) and GaussSum03 packages.

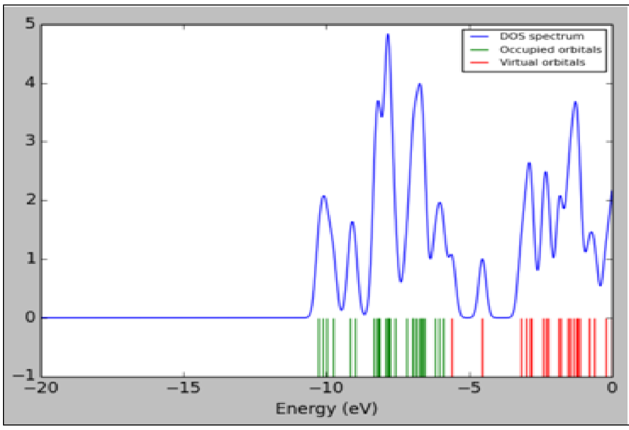

(a) ($3CaTiO_3$)

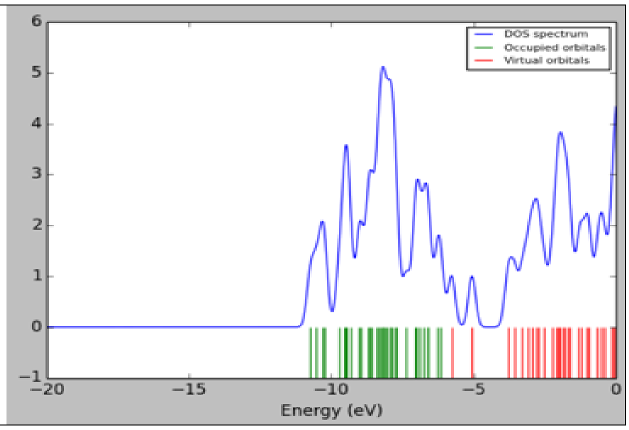

(b) ($3CaTiO_3/TiO_3$

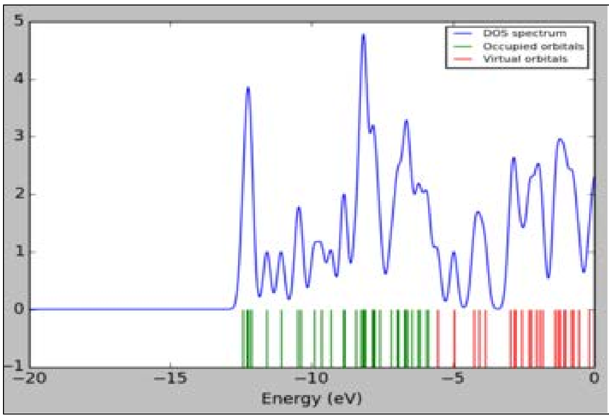

(c) ($3CaTiO_3$)-ZnO

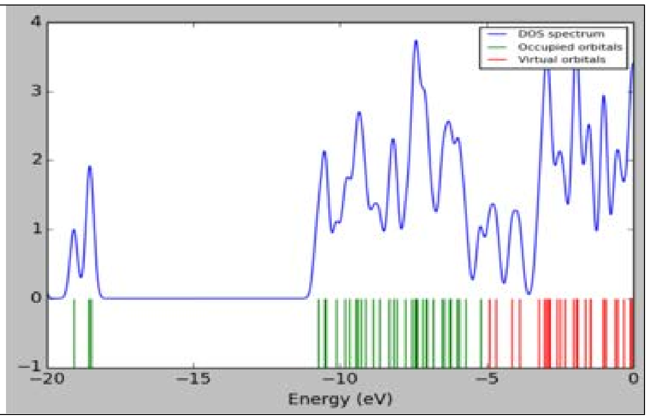

(d) ($3CaTiO_3$)-FeS_2

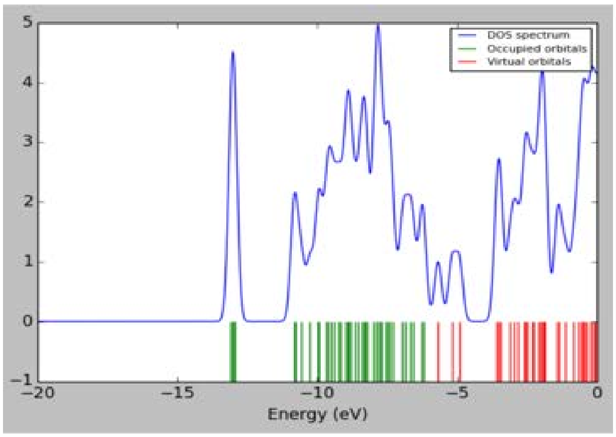

(e) $(3CaTiO_3/TiO_3)$-ZnO

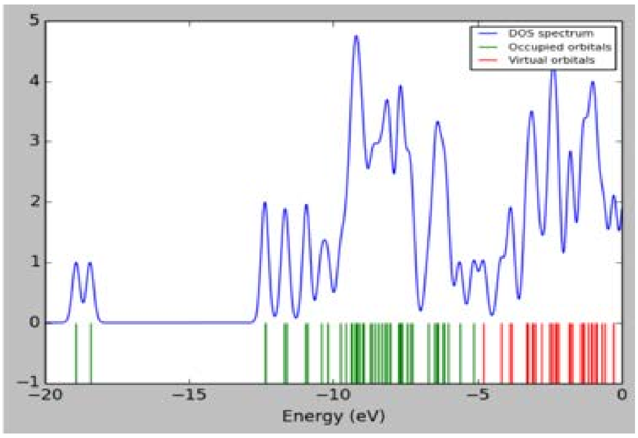

(f) $(3CaTiO_3/TiO_3)$-FeS_2

Fig 4: The density of states for a.**(**$3CaTiO_3$), b.**(**$3CaTiO_3/TiO_3$), c.**(**$3CaTiO_3$)-ZnO, d.**(**$3CaTiO_3$)-FeS_2, e.**(**$3CaTiO_3/TiO_3$)-ZnO and f.**(**$3CaTiO_3/TiO_3$)-FeS_2 systems.

Figure (4) demonstrates that density of state affects because the adsorption procedure of zinc oxide and iron disulfide on the surfaces of **(**$3CaTiO_3$) and **(**$3CaTiO_3/TiO_3$). Therefore, one can assert that the adsorption procedure impact to energy levels density. Simplified comparison between **(**$3CaTiO_3$) and **(**$3CaTiO_3$)-FeS_2 shows that the density of states approximately equal to (4) at the energy approximately (-7 eV), but after the adsorption this value (4) demonstrates at the energy approximately (-12.7 eV). This indicates to new energetic levels can be occupied by electrons at the value (-12.7 eV). So it can be seen that the adsorption of FeS_2 on the nanomaterial surface **(**$3CaTiO_3/TiO_3$) leads to new states can be occupied by electrons, new different peaks appears at new different energies clarify this available energy levels. The density of states is given through the allowed k values that locates in the shell in k space (wave number space), and this yields the allowed states to be occupied by the electrons. The density of states is considered important because it determine if the material metal or non-metal through the energy levels which may be occupied by electrons according to Fermi-Dirac statistics. The density of states also influences by the effective mass of the electron; the density of states increases as the effective mass of electron increase.

Infrared spectra (IR)

The term infrared spectra deal with the interaction between the infrared radiation and the substances. The infrared spectra describe the vibrational modes which be either symmetric or asymmetric. They are symmetric if the atoms that vibrate of the same kind, but the vibration of the atoms of dissimilar kind gives asymmetric mode. The symmetric be either elastic or inelastic [32]. The infrared spectra for **(**$3CaTiO_3$), **(**$3CaTiO_3/TiO_3$), **(**$3CaTiO_3$)-ZnO, **(**$3CaTiO_3$)-FeS_2, **(**$3CaTiO_3/TiO_3$)-ZnO and **(**$3CaTiO_3/TiO_3$)-FeS_2 systems have been inquired by employment density functional theory (DFT) technique at the basis sets 6-31G and B3LYP throughout sophisticated algorithms in Gaussian09 package.

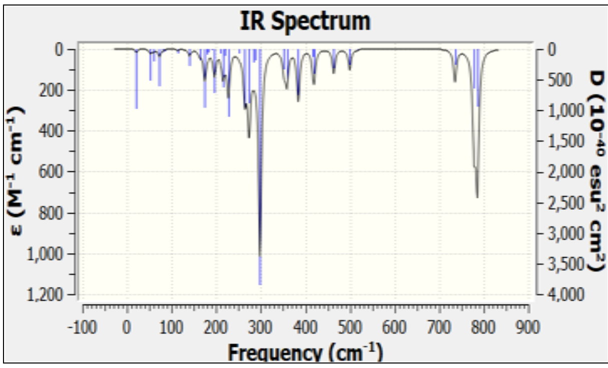

(a) $(3CaTiO_3)$

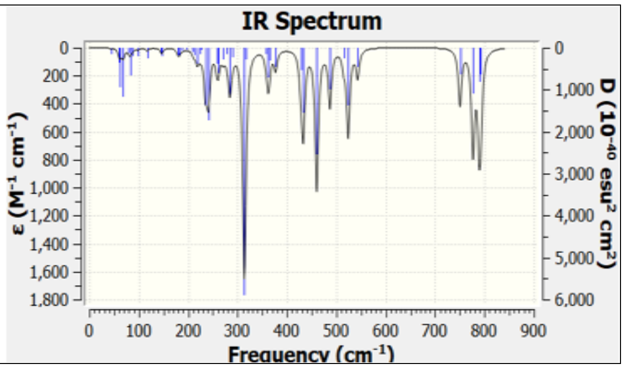

(b) $(3CaTiO_3/TiO_3)$

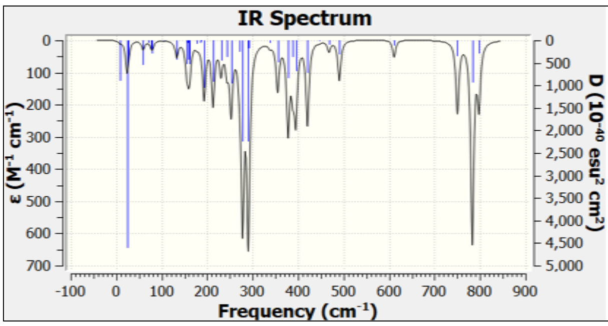

(c) $(3CaTiO_3)$-ZnO

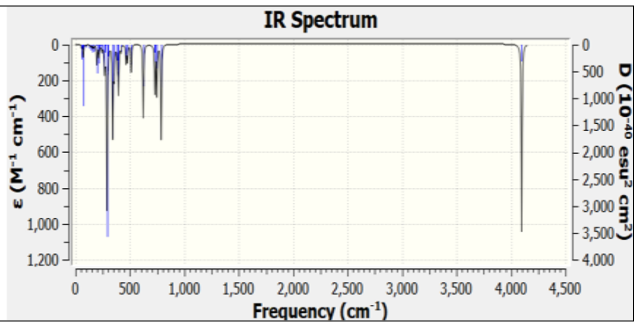

(d) $(3CaTiO_3)$-FeS_2

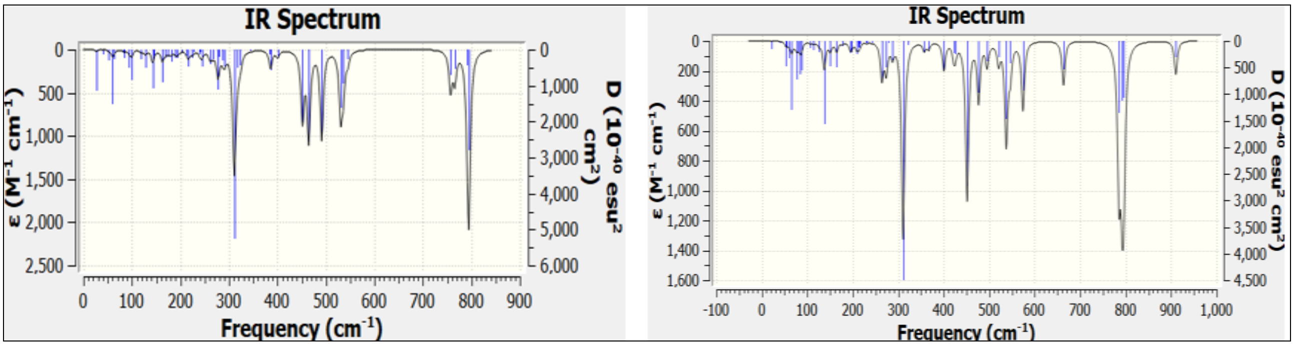

(e) ($3CaTiO_3/TiO_3$)-ZnO **(f)** ($3CaTiO_3/TiO_3$)-FeS_2

Fig (5): The infrared spectra for a.($3CaTiO_3$), b.($3CaTiO_3/TiO_3$), c.($3CaTiO_3$)-ZnO, d.($3CaTiO_3$)-FeS_2, e.($3CaTiO_3/TiO_3$)-ZnO and f.($3CaTiO_3/TiO_3$)-FeS_2 systems.

Figure (5) demonstrates influence the infrared spectra by the adsorption procedure of zinc oxide and iron disulfide on the nanomaterial surfaces **(**$3CaTiO_3$) and **(**$3CaTiO_3/TiO_3$). It can be seen that new bonds originate as a result to the adsorption procedure, but sometimes bonds disappear as a result to shielding procedure. The new bonds in the nanomaterial structure **(**$3CaTiO_3/TiO_3$)-FeS_2 results because the interactions between (iron and sulfur) with (calcium or titanium) atoms. So the new bond that appear in the nanomaterial structure **(**$3CaTiO_3$)-ZnO because the interaction between (sulfur and iron) with (titanium and calcium) atoms. Simple comparison between **(**$3CaTiO_3$) and **(**$3CaTiO_3$)-ZnO shows the peak for **(**$3CaTiO_3$) at the wave number (300 cm^{-1}) is at the intensity (1000 $M^{-1}cm^{-1}$), but the peak at the wave number (300 cm^{-1}) after the adsorption of ZnO on the nanomaterial surface **(**$3CaTiO_3$) appears with intensity at (650 cm^{-1}). The adsorption procedure of iron disulfide on the nanomaterial surface **(**$3CaTiO_3$) leads to new very clear peak at the wave number approximately (4000 cm^{-1}). The infrared spectra are necessary to diagnose the substances throughout the values of the wave numbers that reveals the bonds that result after the interaction.

Conclusions

The molecular geometry of the adsorption procedure can be investigated through density functional theory (DFT) by utilizing Gaussian 09 algorithms. Electrostatic potential pictures demonstrate occurring the adsorption procedure of zinc oxide and iron disulfide on the nanomaterial surfaces **(**$3CaTiO_3$) and **(**$3CaTiO_3$/ TiO_3), the adsorption procedure shows apparently through the electronic charge distribution in the adjacent regions between (ZnO and FeS_2) of one hand and **(**$3CaTiO_3$ and $3CaTiO_3$/ TiO_3) of the other hand. The schematics of density contour maps demonstrate happening the adsorption procedure through the distortion in the shape of contour maps as a result to the interaction between (ZnO and FeS_2) of one hand and **(**$3CaTiO_3$ and $3CaTiO_3$/ TiO_3) on the other hand. The new active regions in the contour maps after the interaction is also prove to occurring the adsorption procedure. The nanomaterial structure ($3CaTiO_3/TiO_3$)-FeS_2 stand for the best donor because it has the minimum value of HOMO energy (-5.1282687 eV), HOMO energy levels are regarded have significance in the study of optical properties of the molecular systems. The values of energy gaps of all nanomaterial structure are in the domain of energy gap of semiconductors, this credit make it acquire an importance in the manufacture of the electronic devices. All nanomaterial structures have polarizability and dipole moment; this credits give the availability to utilize this nanomaterial structures for determination of the optical characteristics of substances. All the nanomaterial structures possess the symmetry (Cs/C_1), the symmetry play an active role in the physical properties of the molecular systems, just like orbitals interactions in order to formation the bonds. The energy gap of ($3CaTiO_3$)-ZnO and ($3CaTiO_3$)-FeS_2 close to (0.30 eV), the energy gaps close to the energy gap of lead telluride (PbTe), this substance (PbTe) has thermoelectric characteristics. The nanomaterial structure ($3CaTiO_3/TiO_3$)-FeS_2 owns ionization potential close to (4.79 eV), it is the minimum value, hence, the nanomaterial structure is the best donor. New active regions appear in IR spectra indicates to new bonds results because the adsorption procedure. New energetic states depict in the diagrams of DOS denotes to new levels can be occupied by electrons.

References

1. Assadi MHN, *et al.* Theoretical study on copper's energetic and magnetism in TiO_2 polymorphs. 2013.
2. Van Maurik T, Gdanitz RJ. A critical note on density functional theory studies on rare-gas dimers. Journal of Chemical Physics. 2002;116(22):9620-9623.
3. Zimmerli U, Parrinello M, Koumoutsakos P. Dispersion corrections to density functionals for water aromatic interactions. Journal of Chemical Physics. 2004;120(6):2693-2699.
4. Grimme S. Semiempirical hybrid density functional with perturbative second-order correlation. Journal of Chemical Physics. 2006;124(3):034108.
5. Orio M, Pantazis DA, Neese F. Density functional theory. Photosynthesis Research. 2009;102:433-453.
6. Sharkas K. Development of new hybrid methods in density functional theory by linear separation of the electron-electron interaction [dissertation]. Paris: Université Pierre et Marie Curie-Paris VI; 2013.
7. Robert J. A critical note on density functional theory studies on rare-gas dimers. Journal of Chemical Physics. 2002;116(22):9620-9623.
8. Carmer CJ. Essentials of Computational Chemistry. Chichester: John Wiley & Sons Ltd; 2002. p. 154-168.
9. Fuchs M, Scheffler M. Computer Physics Communications. 1999.
10. An introduction to computational chemistry using G09W and Avogadro software. Tomberge A. McGill University; 2013.
11. Koch W, Holthausen MC. A Chemist's Guide to Density Functional Theory. 2nd ed. Wiley-VCH Verlag GmbH; 2001.
12. Lee C, Yang W, Parr RG. Development of the Colle-Salvetti correlation energy formula into a functional of

the electron density. Physical Review B. 1988;37:785-789.
13. Burke K. Perspective on density functional theory. Journal of Chemical Physics. 1983;136:150901.
14. Abood HI, *et al*. Study of the effect of electric field on the electronic structure of C_{60}. In: The First Scientific Conference, College of Science; 2013.
15. Anandakumar H, Umamaheswari K. Supervised machine learning techniques in cognitive radio networks during cooperative spectrum handovers. Cluster Computing. 2017;20(2):1505-1515.
16. Navrotsky A. Energetics and crystal chemical systematics among ilmenite, lithium niobate, and perovskite structures. Chemistry of Materials. 1998;10:2787-2792.
17. Abdulsattar MA. Capped ZnO (3,0) nanotubes as building blocks of bare and H-passivated wurtzite ZnO nanocrystals. Superlattices and Microstructures. 2015;85:1-6.
18. Abdulsattar MA. Chlorine gas reaction with ZnO wurtzoid nanocrystals as a function of temperature: A DFT study. Journal of Molecular Modeling. 2017;23(7):221-229.
19. Haiying H, *et al*. Pyrite FeS_2 nanostructures: Synthesis, properties, and applications. Materials Science and Engineering B. 2018;227:104-124.
20. Cotton FA, Wilkinson G, Murillo CA. Advanced Inorganic Chemistry. 6th ed. New York: John Wiley; 1999.
21. DeKock RL, Gray HB. Chemical Bonding and Structure. Menlo Park, CA: Benjamin Cummings; 1980.
22. Annual Reports in Medicinal Chemistry. 1998.
23. Talib SH. Quantum computational study of the electronic properties of the interactions between 3THF and some metallic linear molecules using DFT. Journal of Education for Pure Science - University of Thi-Qar. 2021;11(2):65-72.
24. Sze SM. Semiconductor Devices Physics and Technology. 1990.
25. Jabbar ML. Theoretical study of structural, electronic, and optical properties for graphene nanoribbon with fractal dopants (Al, P, S) [dissertation]. Mustansiriyah University; 2020.
26. Alwan AS. Theoretical study of Na^+ ion, Na atom, and H_2 molecule-Ag and Cu surfaces interaction [dissertation]. 2016.
27. Studying the electronic characteristics and physisorption of OTS on the pure silver surfaces (Ag_{10}), (Ag_{15}), and (Ag_{18}).
28. Hmood MK, Auqla LF. Density functional theory investigation for Ni_6, Co_5, Au_{12}, Y_5, and Ni_6Li, Co_5Li, $Au_{12}Li$, Y_5Na interactions. University of Thi-Qar Journal of Science. 2022;9(2):112-126.
29. Review notes on point group and symmetry. Ohio University; 2017.
30. Hanoon FH, Blawa BD. Density functional theory investigation for sodium atom on copper clusters. International Journal of Science and Research. 2013;2(3):2319-2326.
31. Alwan AS, Hassan AJ, Jabbar ML. Density functional theory (DFT) investigation for pyridazine and pyridazine-P, Al, As, B, C, and In interactions. Iranian Journal of Organic Chemistry. 2020;12(1):2793-2801.
32. Omar MA. Elementary Solid State Physics: Principles and Applications. Lowell Technological Institute; 1975.
33. Alwan AS. Density functional theory investigation of $(C_4H_2N_2)_3$ nanocluster and $(C_4H_2N_2)_3$-P, Al, As, B, C, and In nanoclusters. AIP Conference Proceedings. 2020;2292:030013.

References 2

1. Assadi MH, Hanaor DA. Theoretical study on copper's energetics and magnetism in TiO_2 polymorphs. Journal of Applied Physics. 2013;113(23).
2. Van Mourik T, Gdanitz RJ. A critical note on density functional theory studies on rare-gas dimers. Journal of Chemical Physics. 2002;116(22):9620-9623.
3. Zimmerli U, Parrinello M, Koumoutsakos P. Dispersion corrections to density functionals for water aromatic interactions. Journal of Chemical Physics. 2004;120(6):2693-2699.
4. Grimme S. Semiempirical hybrid density functional with perturbative second-order correlation. Journal of Chemical Physics. 2006;124(3).
5. Orio M, Pantazis DA, Neese F. Density functional theory. Photosynthesis Research. 2009;102:443-453.
6. Sharkas K. Development of new hybrid methods in density functional theory by linear separation of the electron-electron interaction [dissertation]. Paris: Université Pierre et Marie Curie-Paris VI; 2013.
7. Robert J, Van M, Tanja G. A critical note on density functional theory studies on rare-gas dimers. Journal of Chemical Physics. 2002;116(22):9620-9623.
8. Carmer CJ. Essentials of Computational Chemistry. Chichester: John Wiley & Sons Ltd; 2002.
9. Fuchs M, Scheffler M. Ab initio pseudopotentials for electronic structure calculations of polyatomic systems using density-functional theory. Computer Physics Communications. 1999;119(1):67-98.
10. Tomberg A. An introduction to computational chemistry using G09W and Avogadro software. Gaussian 09W Tutorial. 2013.
11. Koch W, Holthausen MC. A Chemist's Guide to Density Functional Theory. John Wiley & Sons; 2015.
12. Lee C, Yang W, Parr RG. Development of the Colle-Salvetti correlation-energy formula into a functional of the electron density. Physical Review B. 1988;37(2):785.
13. Burke K. Perspective on density functional theory. Journal of Chemical Physics. 2012;136(15).
14. Al-Khursan AH, Subhi A, Abood H. Four-wave mixing in long-wavelength III-nitride QD-SOAs. Optik. 2013;124(19):4072-4079.
15. Anandakumar H, Umamaheswari K. Supervised machine learning techniques in cognitive radio networks during cooperative spectrum handovers. Cluster Computing. 2017;20(2):1505-1515.
16. Navrotsky A. Energetics and crystal chemical systematics among ilmenite, lithium niobate, and perovskite structures. Chemistry of Materials. 1998;10(10):2787-2793.
17. Abdulsattar MA. Capped ZnO (3,0) nanotubes as building blocks of bare and H-passivated wurtzite ZnO nanocrystals. Superlattices and Microstructures. 2015;85:813-819.
18. Abdulsattar MA. Chlorine gas reaction with ZnO wurtzoid nanocrystals as a function of temperature: A DFT study. Journal of Molecular Modeling. 2017;23(4):125.
19. Qin H, Jia J, Lin L, Ni H, Wang M, Meng L. Pyrite FeS_2 nanostructures: Synthesis, properties, and applications. Materials Science and Engineering B. 2018;236:104-124.

20. Cotton FA, Wilkinson G, Murillo CA, Bochmann M. Advanced Inorganic Chemistry. John Wiley & Sons; 1999.
21. DeKock R, Gray H. Chemical Bonding and Structure. Benjamin/Cummings Publishing Inc.; 1980.
22. Bristol JA, Doherty AM. Annual Reports in Medicinal Chemistry. Academic Press; 1998.
23. Alwan AS, Talib SH. Quantum computational study of the electronic properties of the interactions between 3THF and some metallic linear molecules using DFT. Journal of Education for Pure Science - University of Thi-Qar. 2021;11(2):53-67.
24. Sze SM. Semiconductor Devices: Physics and Technology. John Wiley & Sons; 2008.
25. Jabbar ML, Al-Shejairy KJ. Uma nova geometria fractal doping para nanofibras de grafeno e a otimização de cristal: Um estudo da teoria da densidade funcional (DFT). Periódico Tchê Química. 2020;17(35).
26. Alwan AS. Theoretical study of Na^+ ion, Na atom, and H_2 molecule-Ag and Cu surfaces interaction [dissertation]. Baghdad: Al Mustansiriyah University; 2016.
27. Ahmed AB. Studying the electronic characteristics and physisorption of OTS on the pure silver surfaces (Ag_{10}), (Ag_{15}), and (Ag_{18}). University of Thi-Qar Journal of Science. 2023;10(2):151-9.
28. Hommod MK, Auqla LF. Density functional theory investigation for Ni_6, Co_5, Au_{12}, Y_5 and Ni_6Li, Co_5Li, $Au_{12}Li$, Y_5Na interactions. University of Thi-Qar Journal of Science. 2022;9(2):105-112.
29. Lesk AM. Introduction to Symmetry and Group Theory for Chemists. Springer; 2004.
30. Hassan F, Daraam B, Shwya A. Density functional theory investigation for sodium atom on copper clusters. International Journal of Science and Research. 2015.
31. Omar MA. Elementary Solid State Physics: Principles and Applications. Pearson Education India; 1999.
32. Alwan AS. Density functional theory investigation of $(C_4H_2N_2)_3$ nanocluster and $(C_4H_2N_2)_3$-P, Al, As, B, C, and In nanoclusters. AIP Conference Proceedings. 2020;2292(1).